

Electron Density of Orthoboric Acid Determined by X-ray Diffraction at 105 K and *ab initio* Calculations

BY MICHAEL GAJHEDE, SINE LARSEN AND STEN RETTRUP

Department of Physical Chemistry, H. C. Ørsted Institute, University of Copenhagen, Universitetsparken 5, DK-2100 Copenhagen Ø, Denmark

(Received 24 January 1986; accepted 20 June 1986)

Abstract

The charge distribution in orthoboric acid, $B(OH)_3$, $M_r = 61.83$, has been investigated experimentally using low-temperature X-ray diffraction data and theoretically by *ab initio* calculations. Crystal data at 105 K, triclinic, space group $P\bar{1}$, $a = 7.0187(14)$, $b = 7.035(2)$, $c = 6.3472(12)$ Å, $\alpha = 92.49(12)$, $\beta = 101.46(2)$, $\gamma = 119.76(2)^\circ$, $V = 262.90(1)$ Å³, $Z = 4$, $D_x = 1.562(1)$ g cm⁻³, Mo $K\alpha$, $\lambda = 0.71073$ Å, $\mu = 1.51$ cm⁻¹, $F(000) = 128$, $R = 0.038$ for 3370 observed reflections. The two independent $B(OH)_3$ molecules are identical and planar, each having threefold symmetry. $\langle B-O \rangle = 1.368(1)$ Å, $\langle O-B-O \rangle = 120.00(7)^\circ$. The structural parameters for B and O, determined from high-order refinement, are virtually identical to those obtained from a multipole refinement using all the data. The static deformation density in the B-O bonds as determined from a multipole refinement agrees well with the theoretical deformation density obtained from an *ab initio* calculation beyond the Hartree-Fock level, which had peaks with a density of 0.3 e Å⁻³. The features around the O atoms, especially in the lone-pair regions, agree less well.

1. Introduction

Chemical bonding in compounds containing the heavier elements (C, N, O) of the first-eight period of the Periodic Table has been thoroughly investigated in numerous experimental charge-density studies. Relatively few similar studies have been undertaken for the electron-deficient compounds that are formed with the lighter (Be, B) elements in the period. Kirfel, Will & Stewart (1983) studied the charge density in $LiBO_2$, and found that the three different B-O bonds not only differed in length but also in their experimental deformation densities.

Orthoboric acid is very suited for an experimental investigation of the charge density in B-O bonds by X-ray diffraction methods. In one of the first accurate structure determinations, Zachariasen (1954) showed that the two molecules in the asymmetric unit are identical, and that both possess a threefold axis. This result was later confirmed by Craven & Sabine (1966)

who studied an isotope-substituted form of orthoboric acid, $^{11}B(OD)_3$, by neutron diffraction to obtain detailed information about the hydrogen bonding.

Fig. 1 illustrates how the $B(OH)_3$ molecules are linked by hydrogen bonds in layers almost perpendicular to the c axis.

The deformation density in the B-O-H moiety can thus be studied in six chemically equivalent, but crystallographically different, units. $B(OH)_3$ contains only first- and second-row elements, which results in a high ratio between valence and core electrons. Furthermore, the effects of anomalous dispersion and absorption are insignificant.

Orthoboric acid is also suited for a theoretical investigation of the charge density by *ab initio* methods. The experimental results showed that to a good approximation C_{3h} symmetry can be imposed on the molecule. This makes it possible to perform theoretical calculations to a relatively high precision. Gupta & Tossell (1981) and Gundersen (1981) have earlier determined the deformation density in orthoboric acid using a basis set of double- ζ quality at the Hartree-Fock level.

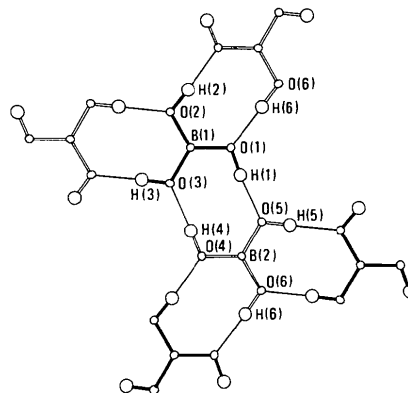


Fig. 1. An ORTEP drawing (Johnson, 1976) showing a layer of hydrogen-bonded $B(OH)_3$ molecules viewed along the c axis. To distinguish between the two crystallographically independent molecules, molecule (II) [B(2), O(4), O(5), O(6)] is drawn with open bonds. The lines indicate the hydrogen bonds in the structure.

In this paper, we report an investigation of the charge density in $\text{B}(\text{OH})_3$ from low-temperature X-ray diffraction data and by *ab initio* calculations from CI (configuration interaction) wavefunctions. The hydrogen bonding in $\text{B}(\text{OH})_3$ has earlier been investigated theoretically by Yamabe, Kitaura & Nishimoto (1978). They performed *ab initio* calculations for a boric acid dimer using only an STO-3G minimal basis set.

2. Experimental

2.1 X-ray crystallography

Single crystals were grown from aqueous solution in a desiccator over H_2SO_4 . X-ray diffraction data were collected with an Enraf-Nonius CAD-4 diffractometer. $\text{Mo K}\alpha$ radiation ($\lambda = 0.71073 \text{ \AA}$) was obtained from a graphite monochromator. The crystal ($0.08 \times 0.10 \times 0.15 \text{ mm}$) was cooled by a nitrogen-gas stream to 105 K by an Enraf-Nonius low-temperature device. The temperature of the gas stream was monitored by a thermocouple; the variations of the temperature were within 1 K. The unit-cell parameters were determined from a least-squares refinement using 20 reflections with $19.26 < \theta < 21.95^\circ$. The effect of cooling is highly anisotropic. The c axis is reduced by 0.2 \AA but the other cell dimensions are virtually unchanged.

After a detailed profile analysis of nine selected reflections, the $\omega/2\theta$ -scan type was chosen. The scan width was increased by 25% on each side of the peak to define the background. The intensities were recorded at 96 equal intervals. For reflections with $\theta < 30^\circ$, $\Delta\omega = 1.5^\circ + 0.35^\circ \tan \theta$ and a maximum scan time of 240 s were used. Data with $\theta > 30^\circ$ had $\Delta\omega = 1.3^\circ + 0.35^\circ \tan \theta$ and a maximum scan time of 180 s.

During the data collection, which lasted six weeks, the intensities of three standard reflections were recorded every 10 000 s. No systematic decrease in the intensities of these reflections was observed; the fluctuations were within 5.5% of the averaged intensity. The orientation of the crystal was checked by determination of the setting angles for every 100 reflections.

15 761 reflections in a full sphere, $\sin \theta/\lambda < 1.16 \text{ \AA}^{-1}$, were measured ($-16 < h < 16$, $-16 < k < 16$, $-14 < l < 14$). 3372 had negative intensities and 6470 were considered unobserved, based on a $2\sigma(I)$ criterion. For nine reflections with a strongly asymmetric background, two times the smallest background was used to define the background. The observed peak position differed by more than 0.2° from the calculated value for 14 observed reflections. An attenuator with the filter factor 17.96 was used in measuring the intensities of five strong reflections. The intensities for the standard reflections showed some significant fluctuations. To correct for these long-term instabilities a scale factor $K(t)$ was applied

to the net intensity. This scale factor was determined by a method similar to the one described by Dam, Harkema & Feil (1983). Cubic spline functions were used to fit the intensity of each standard reflection. The contribution to the correction factor $K(t)$ from each standard reflection was given a weight inversely proportional to the distance in reciprocal space between the standard reflection and the reflection measured at time t . The correction factors $K(t)$ ranged from 0.97 to 1.02.

In accordance with the analysis made by Rees (1977) and the results of Seiler, Schweizer & Dunitz (1984), the variance of the integrated intensity was expressed as: $\text{var}(I) = \text{var}(I)_{\text{counting}} + (pI)^2$, where $\text{var}(I)_{\text{counting}}$ is the variance calculated from counting statistics. Analysis of the standard reflections, of the ψ scans for 12 reflections and of the reflections measured at least four times, indicated that $p = 0.02$ gave the best fit of the variance. The data were corrected for Lorentz, polarization and absorption effects ($\mu = 1.51 \text{ cm}^{-1}$). The last correction was performed by a numerical Gaussian integration over the crystal volume (Coppens, Leiserowitz & Rabinovich, 1965). The transmission factors were in the range 0.98–0.99. The absorption correction had no significant effect on the internal R value.

The ψ scans revealed that a few low-angle reflections were affected by anisotropic extinction. The largest variation in these scans was 8%. An inspection of the data showed that only eight reflections were noticeably affected by extinction. As the data set is extensive, the choice was made to exclude these reflections from the data. The symmetry-related reflections were averaged ($R_{\text{int}} = 0.0151$). During the refinements an analysis of the data showed that the reflections with $1.10 \leq \sin \theta/\lambda \leq 1.16 \text{ \AA}^{-1}$ were of poorer quality. Inclusion of these in the calculations only tended to increase the noise level. It was decided to exclude them from the data. Of the resulting 6721 reflections, 3377 had $I > 2\sigma(I)$ and these were used in the final calculations and refinements.

2.2 *Ab initio* calculations

In the theoretical calculations, the $\text{B}(\text{OH})_3$ molecule was assumed to possess C_{3h} symmetry. The molecular dimensions were averaged from the neutron diffraction results (Craven & Sabine, 1966), and the H atoms were placed in the plane of the BO_3 group. The boric acid dimer has C_{2h} symmetry and is formed by two boric acid molecules with the geometry of the monomer and linked by two linear hydrogen bonds with an $\text{O}\cdots\text{O}$ separation of 2.713 \AA .

All calculations were performed in the SCF LCAO MO description using two different Gaussian-type contracted basis sets. A double- ζ basis (B, O/9, 5, H/4) contracted to (B, O/4, 2, H/2) as given by Dunning (1970) was used for $\text{B}(\text{OH})_3$ and

[B(OH)₃]₂. Calculations on B(OH)₃ were also undertaken using an extended basis set, which improved the description of the core and valence regions. The basis set contained *d*-polarization functions at B and O and *p*-polarization functions at H, (B, O/11, 6, 1, H/4, 1) contracted to (B, O/5, 4, 1, H/2, 1) (Dunning, 1971). The orbital exponents for the polarization functions were 0.75 for B, 0.85 for O and 1.16 for H. The calculations were performed using the *MOLECULE* (Almløf, 1974)–*ALCHEMY* (Bagus, 1971)–*ENERGY* (Rettrup & Sarma, 1977) program package.

In the CI calculations on B(OH)₃, all single and double excitations were included from the Hartree–Fock ground state, excluding excitations from the four lowest core orbitals and with a total of nine virtual orbitals giving rise to 3265 configuration state functions of ¹A' symmetry of C_s.

3. Results and discussion

3.1 High-order data refinement

Least-squares refinements were performed, minimizing the error function $\sum w[F_o(H) - kF(H)]^2$ using the *XRAY76* system (J. M. Stewart, 1976), $w = 1/\sigma^2(F)$. Starting values for positional and thermal parameters were taken from Zachariasen's (1954) room-temperature results. The atomic scattering factors for B and O were taken from Cromer & Mann (1968), and for H from Stewart, Davidson & Simpson (1965). The corrections due to the anomalous dispersion calculated by Cromer & Liberman (1970) were included in the scattering factors for B and O. A refinement based on the full data set converged at residuals of $R = 0.038$ and $wR = 0.044$.

The positional and thermal parameters were determined from refinements using reflections measured at high scattering angles. Different refinements were performed, where the minimum $\sin \theta/\lambda$ value was changed at intervals of 0.05 \AA^{-1} between 0.50 and 0.95 \AA^{-1} . When the minimum $\sin \theta/\lambda$ values were larger than 0.5 \AA^{-1} , the thermal parameters for the H atoms took on physically unrealistic values. Consequently, the parameters of the H atoms were only included in the refinement with $\sin \theta/\lambda = 0.5 \text{ \AA}^{-1}$. This refinement included 97 variables, and converged at the residuals $R = 0.034$, $wR = 0.030$ and $S = 1.085$. Though the parameters determined for the H atoms from the refinement were assumed to represent the correct direction of the O–H bond, the corresponding bonds are too short. Instead we chose to fix the H atoms at positions corresponding to the same direction but with their O–H distance elongated to 0.97 \AA , the O–D bond length found by Craven & Sabine (1966). The thermal parameters for the H atoms were fixed at a value at 0.02 \AA^2 .

An analysis of the refinement results showed that the effects of the bonding and valence electrons were

insignificant when the reflections with $\sin \theta/\lambda \leq 0.80 \text{ \AA}^{-1}$ were excluded from the calculations. Using the 1673 reflections with $0.80 < \sin \theta/\lambda < 1.16 \text{ \AA}^{-1}$, a refinement of 73 variables, which included the scale factor, positional and thermal parameters, parameters for the non-H atoms had converged when the maximum shift/e.s.d. in the parameters was 0.08. The maximum and minimum peaks in the final $\Delta\rho$ map were 0.70 and -0.70 e \AA^{-3} . The residuals after this calculation were $R = 0.042$, $wR = 0.040$ and $S = 1.004$. The resulting atomic parameters from this refinement are listed in Table 1.*

3.2 Multipole refinement

The rigid-pseudoatom model of R. F. Stewart (1976) with atomic scattering factors expanded by spherical harmonics (Hansen & Coppens, 1978) was used to describe the charge density in the crystal. The core atomic scattering factors for B and O were taken from *International Tables for X-ray Crystallography* (1974). The spherical valence scattering factors for B and O were calculated as the difference between the total scattering factor by Cromer & Mann (1968) and the core contribution. For H, the values found by Stewart *et al.* (1965) were used. Multipole expansions were included up to octapoles for B and O. For H a single dipole was used. The parameters for the H atoms were fixed at the same values as those used for the high-order refinement. Following a suggestion by R. F. Stewart (1976), the exponents in the radial functions were all chosen so that the densities on the nuclei satisfied Poisson's equation. The local coordinate systems were oriented in the same way for each B–O–H entity. The refinements with *MOLLY* (Hansen & Coppens, 1978) were performed using the 3377 reflections in the full data set. The non-crystallographic C_{3h} symmetry of the molecules was obvious in these refinements. The only multipole functions for B that had population parameters greater than two e.s.d.'s were those that are allowed in C_{3h} symmetry, and only these parameters were included in the final refinements. 189 variables were included in refinement cycles. The final residuals are $R = 0.023$, $wR = 0.025$ and $S = 1.13$. The positional and thermal parameters obtained from this refinement are listed in Table 1 for comparison. The population parameters used in the description of the densities of the independent O and B atoms were very similar. In Table 2, averaged values of the population parameters with the mean standard deviation from the least-squares refinement as well as the statistical standard deviation are given.

* Lists of structure factors and two further deformation-density maps have been deposited with the British Library Document Supply Centre as Supplementary Publication No. SUP 43100 (19 pp.). Copies may be obtained through The Executive Secretary, International Union of Crystallography, 5 Abbey Square, Chester CH1 2HU, England.

Table 1. Atomic parameters for orthoboric acid

Parameters from high-order refinement (first line) and multipole refinement (second line). Displacement parameters for H atoms only given from multipole refinement. In high-angle refinement, a fixed value of 0.02 \AA^2 was used.

	<i>x</i>	<i>y</i>	<i>z</i>	U_{11}^*	U_{22}	U_{33}	U_{12}	U_{13}	U_{23}
B(1)	0.64860 (12)	0.42643 (12)	0.26043 (16)	0.0088 (2)	0.0079 (2)	0.0154 (3)	0.0050 (2)	0.0048 (2)	0.0032 (2)
	0.64844 (6)	0.42648 (6)	0.26038 (6)	0.0087 (1)	0.0079 (1)	0.0156 (2)	0.0050 (1)	0.0048 (1)	0.0034 (1)
B(2)	0.30896 (12)	0.75819 (11)	0.23916 (15)	0.0078 (2)	0.0073 (2)	0.0150 (3)	0.0040 (2)	0.0033 (2)	0.0022 (2)
	0.30894 (6)	0.75823 (6)	0.23940 (5)	0.0078 (1)	0.0074 (1)	0.0155 (2)	0.0041 (1)	0.0034 (1)	0.0023 (1)
O(1)	0.42575 (9)	0.30116 (9)	0.26380 (13)	0.0082 (1)	0.0089 (1)	0.0220 (3)	0.0047 (1)	0.0059 (1)	0.0040 (1)
	0.42559 (3)	0.30116 (4)	0.26361 (4)	0.0083 (1)	0.0094 (1)	0.0223 (1)	0.0050 (1)	0.0058 (1)	0.0041 (1)
O(2)	0.77240 (9)	0.32667 (8)	0.25093 (12)	0.0091 (1)	0.0079 (1)	0.0205 (2)	0.0051 (1)	0.0059 (1)	0.0032 (1)
	0.77245 (4)	0.32657 (4)	0.25137 (4)	0.0093 (1)	0.0080 (1)	0.0209 (1)	0.0053 (1)	0.0059 (1)	0.0032 (1)
O(3)	0.74622 (10)	0.65016 (9)	0.26318 (15)	0.0108 (2)	0.0076 (1)	0.0266 (3)	0.0054 (1)	0.0084 (2)	0.0057 (2)
	0.74654 (4)	0.65032 (4)	0.26327 (4)	0.0111 (1)	0.0079 (1)	0.0264 (1)	0.0056 (1)	0.0085 (1)	0.0057 (1)
O(4)	0.53521 (9)	0.88525 (9)	0.24894 (13)	0.0075 (2)	0.0082 (2)	0.0221 (3)	0.0039 (1)	0.0045 (1)	0.0035 (2)
	0.53531 (4)	0.88530 (4)	0.24873 (4)	0.0076 (1)	0.0083 (1)	0.0223 (1)	0.0040 (1)	0.0046 (1)	0.0035 (1)
O(5)	0.21322 (9)	0.53555 (9)	0.24351 (31)	0.0088 (1)	0.0073 (1)	0.0209 (3)	0.0043 (1)	0.0053 (1)	0.0036 (1)
	0.21313 (4)	0.53531 (4)	0.24336 (4)	0.0089 (1)	0.0073 (1)	0.0211 (1)	0.0041 (1)	0.0053 (1)	0.0036 (1)
O(6)	0.17963 (9)	0.85396 (9)	0.22843 (13)	0.0093 (1)	0.0089 (1)	0.0262 (3)	0.0058 (1)	0.0056 (1)	0.0032 (1)
	0.17974 (4)	0.85407 (4)	0.22874 (4)	0.0096 (1)	0.0088 (1)	0.0242 (1)	0.0058 (1)	0.0058 (1)	0.0034 (1)
H(1)	0.3606	0.3931	0.2662	0.013 (4)					
H(2)	0.6848	0.1714	0.2582	0.009 (3)					
H(3)	0.9012	0.7201	0.2542	0.016 (3)					
H(4)	0.6106	0.8022	0.2631	0.007 (3)					
H(5)	0.0580	0.4630	0.2513	0.019 (4)					
H(6)	0.2619	1.0132	0.2362	0.018 (3)					

* Displacement parameters (in \AA^2) of the form $\exp[-2\pi^2(h^2a^{*2}U_{11} + k^2b^{*2}U_{22} + \dots + 2klb^*c^*U_{23})]$.

3.3 Theoretical calculations

A comparison between different types of calculations performed for B(OH)_3 (Gajhede, 1985) showed that the derived deformation density was improved more by enlargement of the basis set than by performing CI calculations with a small basis set. It is remarkable, however, that the population analyses for the SCF and CI calculations gave different charges on the B atom but very similar π occupations (0.4). The deformation densities were calculated as the difference between the total density and the spherically averaged SCF atomic ground-state densities calculated with the same contracted basis set. An estimate of the net charge for the atoms in B(OH)_3 can be obtained as the difference between the multipole population parameter for the monopole for the pseudoatoms B, O and H and the formal valence charge. From the values in Table 2, the charges B(0.83), O(-0.69) and H(0.41) are determined which are in good agreement with the gross atomic charges calculated by Gajhede (1985).

3.4 Refinement results

The two sets of positional and thermal parameters listed in Table 1, obtained by the high-order and multipole refinements respectively, are virtually identical. The *x* coordinate for O(3) has the maximum difference of 3.4σ . Hirshfeld's (1976) rigid-bond postulate was used to test the physical reliability of the displacement parameters for the non-H atoms obtained by the high-order refinement. The displacement parameters for the two crystallographically

Table 2. Population parameters for orthoboric acid

Multipole population parameters are averaged over all atoms in the asymmetric unit. First number in parentheses is the average of the e.s.d.'s from the least-squares refinement, second number is the statistical standard deviation. Only multipoles populated by more than two times the average standard deviation are included.

	B	O	H
ρ_v	2.17 (3) (3)	6.69 (2) (13)	0.59 (3) (5)
d_1			0.29 (3) (7)
d_2			0.08 (3) (7)
d_3			-0.12 (3) (10)
q_1	-0.189 (10) (3)	-0.07 (1) (2)	
q_2			
q_3			
q_4		0.03 (1) (5)	
q_5			
o_1			
o_2			
o_3		0.028 (8) (40)	
o_4			
o_5	0.22 (2) (1)		
o_6		0.142 (9) (16)	
o_7	-0.14 (2) (3)	-0.045 (9) (4)	

independent molecules are very similar. The displacements of B along the B-O bonds are in the range $68\text{--}79 \times 10^{-4} \text{ \AA}$; these are almost the same as the equivalent displacements of the O atoms, $62\text{--}72 \times 10^{-4} \text{ \AA}$.

The bond lengths and angles calculated from the high-order parameters are given in Table 3. The two B(OH)_3 molecules are identical and both possess a threefold symmetry axis. The molecular dimensions are in excellent agreement with the averaged dimensions for the B-O-H moiety, determined from

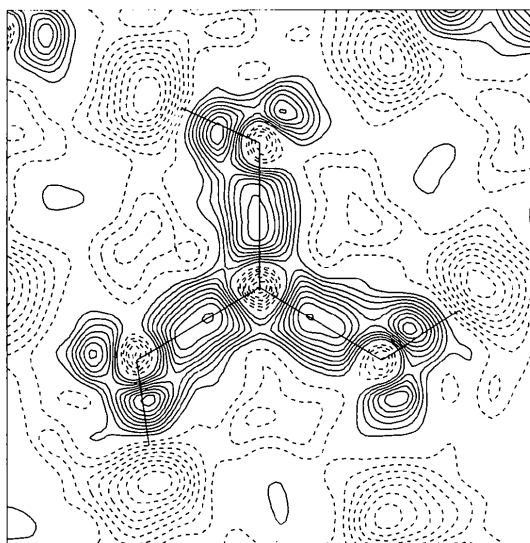
the room-temperature neutron diffraction study ($\langle B-O \rangle = 1.367 \text{ \AA}$, $\langle O-B-O \rangle = 120.0^\circ$) (Craven & Sabine, 1966). The BO_3 moieties are planar, B having the maximum deviation from the least-squares plane in both molecules, 0.005 \AA . The H atoms are twisted slightly out of the BO_3 planes. The dihedral angles $O-B-O-H$ are in the range -4 to 6° , corresponding to hydrogen distances from the least-squares BO_3 plane between 0.02 and 0.09 \AA . Craven & Sabine (1966) suggested that these small tilts are caused by the intermolecular hydrogen bonds.

Table 3. Bond lengths (\AA) and bond angles ($^\circ$) calculated from parameters obtained from the high-order refinement

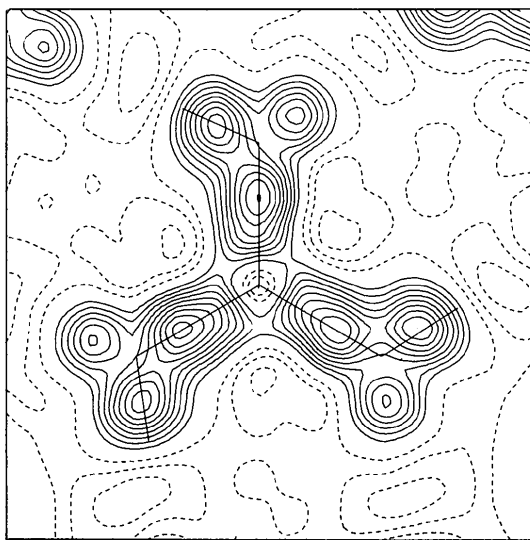
B(1)-O(1)	1.368 (1)	B(2)-O(4)	1.368 (1)
B(1)-O(2)	1.369 (1)	B(2)-O(5)	1.368 (1)
B(1)-O(3)	1.367 (1)	B(2)-O(6)	1.367 (1)
O(1)-B(1)-O(2)	119.82 (6)	O(4)-B(2)-O(5)	119.79 (8)
O(2)-B(1)-O(3)	120.17 (7)	O(5)-B(2)-O(6)	120.09 (7)
O(1)-B(1)-O(3)	120.00 (9)	O(4)-B(2)-O(6)	120.11 (7)

3.5 Deformation densities

The X-ray diffraction data were used to calculate deformation densities. The coefficients in the Fourier series were $F_o - F_c$, where F_c is the structure factor calculated for a procrystal containing neutral spherical atoms with positional and thermal parameters obtained from refinements using the high-order data. The deformation densities around the six equivalent B-O-H units show identical features in accordance with the symmetry of the $B(OH)_3$ molecule. The differences between the groups are of the same order of magnitude as the errors in the maps. Consequently, the densities in the six crystallographically different B-O-H groups were averaged to reduce the noise level. This averaged map is reproduced in Fig. 2(a). Two maps showing the deformation densities in the two different BO_3 planes have been deposited. In a map similar to Fig. 2(a), based on data with $\sin \theta/\lambda < 0.8 \text{ \AA}^{-1}$, the electron density in the O-H-bond region was considerably reduced. In an attempt to avoid series-termination effects, a Dirac-Fermi distribution function was applied to F_o and F_c which reduced the function values to 50% at

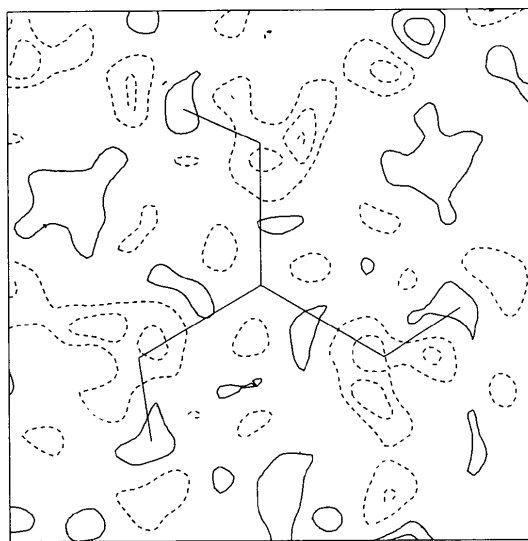


(a)



(b)

Fig. 2. Averaged experimental densities in the BO_3 plane. Based on reflections with $\sin \theta/\lambda \leq 1.10 \text{ \AA}^{-1}$. (a) Deformation density based on the parameters derived from the high-order refinement. (b) Dynamic-model map calculated from the parameters obtained by the multipole refinement.



(c)

Fig. 2 (cont.). (c) Residual density showing the difference between the experimental and the dynamic map. The contours are drawn at intervals of $0.05 e \text{ \AA}^{-3}$, the zero contour is omitted.

$\sin \theta/\lambda$ equal to 0.8 \AA^{-1} and to 10% at 1.0 \AA^{-1} . The map produced with these coefficients was not significantly different from the one produced with a resolution of 0.8 \AA^{-1} .

The threefold symmetry of the $\text{B}(\text{OH})_3$ molecules was also obvious from the multipole refinements. The dynamic-model deformation density (Coppens, 1982) presented in Fig. 2(b) is calculated from the parameters derived from the multipole refinement, averaged over the six B–O–H groups.

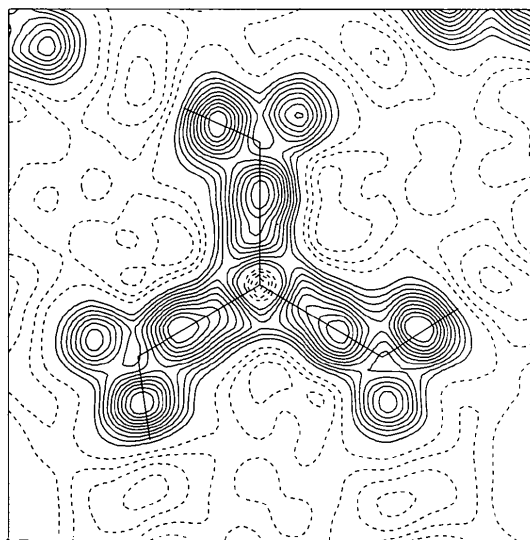
The density in the B–O bond is very similar in the two maps illustrated in Figs. 2(a) and 2(b). The main differences are around O; there is relatively more

density in the O–H bond than in the lone-pair region in the model map. An averaged residual map was calculated with the coefficients $F_o - F_{\text{cmul}}$, where F_{cmul} is the set of structure factors calculated from the multipole model. The resulting map is depicted in Fig. 2(c). This map shows that the actual multipole expansion fits the region around O less satisfactorily than the region around B. The most populated multipole on O is the octapole giving a trigonal charge distribution. However, the experimental charge density around O is not completely trigonal since the angle B–O–H is 113.3° .

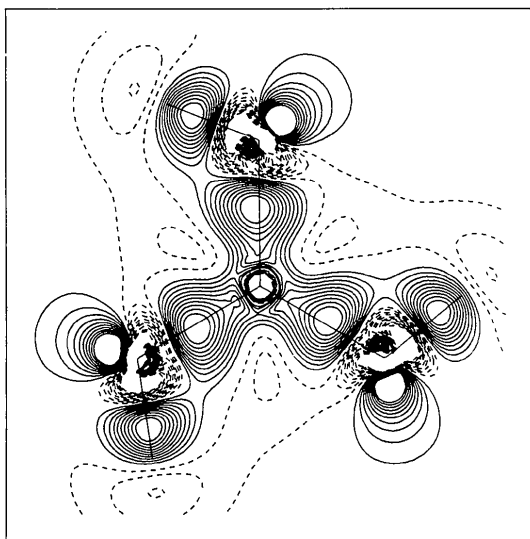
In order to be able to compare experimental and theoretical deformation densities more quantitatively, it is necessary either to perform a thermal smearing of the theoretical density, or to calculate a static-model map (Coppens, 1982). The latter approach was chosen for orthoboric acid, since comparison of experimental and theoretical results for urea (Swaminathan, Craven, Spackman & Stewart, 1984) had shown that the static deformation density deconvoluted from thermal motion is satisfactorily represented by R. F. Stewart's (1976) pseudoatom model. The static deformation density map is shown in Fig. 3(a). The theoretical deformation density map is presented in Fig. 3(b). A charge-density deformation map obtained from a double- ζ HF-SCF calculation was identical to the map presented by Gupta & Tossell (1981). This map agrees less well with the experimental deformation density than the map shown in Fig. 3(b). The main effects of including polarization functions and configuration interaction into the computations are to move charge from the O lone pair into the B–O-bond region. The errors in the theoretical maps are greatest near the cusps of the atoms, and in Fig. 3(b) relatively large holes are observed at the atomic sites. This is probably related to the use of Gaussian functions.

The density in the B–O bond region is very similar in the two maps shown in Fig. 3, both qualitatively and quantitatively. The relative position of the deformation density peak in the O–H bond is shifted towards H in the theoretical map, but the peak heights are similar. The lone-pair density of O exhibits the greatest discrepancies between the theoretical and experimental densities. The difference between the peak heights is so large that it cannot only be due to the insufficient description of the lone pair in the model map but basis-set effects may also be of importance. Furthermore, the lone-pair peaks appear at a distance of *ca* 0.5 \AA from the O atom in the experimental maps. In the theoretical deformation densities, the lone-pair peak is closer to the O (0.4 \AA).

Kirfel, Will & Stewart (1983) have studied the chemical bonding in LiBO_2 . In this metaborate salt, the three different B–O bonds differ both in length and in the features of their experimental deformation densities. Compared with $\text{B}(\text{OH})_3$, the charge



(a)



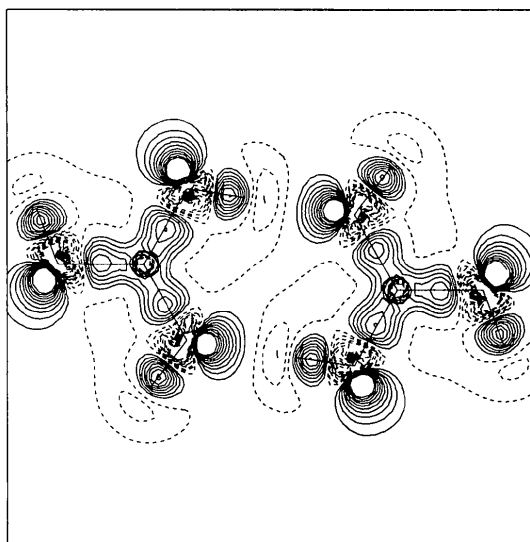
(b)

Fig. 3. (a) Static-model map calculated from the pseudoatom model with atoms at rest. (b) Theoretical deformation density map calculated from an *ab initio* HF SCF CI calculation. The maps are drawn as described under Fig. 2.

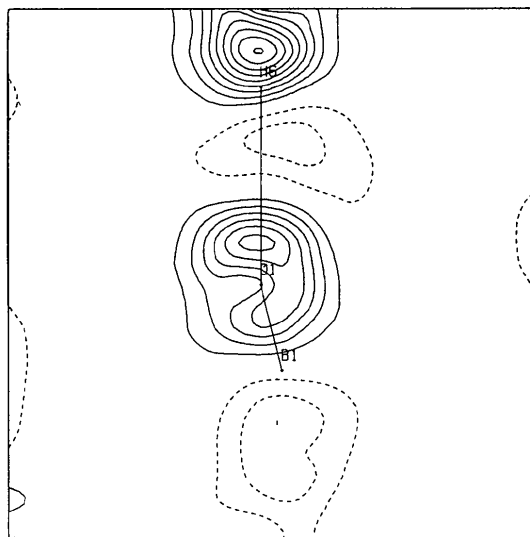
accumulation is slightly larger both in the B–O bonds ($0.5\text{--}0.7\text{ e \AA}^{-3}$) and in the O lone pairs for the negatively charged BO_3 unit.

3.6 Hydrogen bonding in $\text{B}(\text{OH})_3$

As part of an IUCr project, the charge density in oxalic acid dihydrate was investigated extensively using both theoretical and experimental techniques (Coppens, 1984). In this study the biggest differences between the theoretical and experimental deformation densities are found in the O lone-pair region.



(a)



(b)

Fig. 4. (a) Theoretical deformation map calculated for the orthoboric acid dimer based on a HF SCF calculation. (b) Static-model map showing the deformation density in the $\text{O}(1)\text{--H}(1)\cdots\text{O}(6)$ hydrogen bond. The maps are drawn as described under Fig. 2.

The theoretical maps produce less diffuse and higher densities in the lone-pair region than the experimental maps, which may be caused by the limited basis set. From the results of theoretical calculations, it has also been suggested (Hermansson, 1984) that the origin of this difference between theoretical and experimental densities is intermolecular interactions, e.g. hydrogen bonding in the crystal.

In the theoretical and experimental densities for $\text{B}(\text{OH})_3$, the same discrepancy for the density in the O lone pair is observed. A model map is given in Fig. 4(a) which shows the deformation density in the $\text{O}(1)\text{--H}(6)$ hydrogen bond (see Fig. 1), in a plane orthogonal to the $\text{B}(1)\text{--O}(1)\text{--O}(2)\text{--O}(3)$ group. Though the O lone pair is directed towards H(6), the peak is not exactly on the line $\text{O}(1)\text{--H}(6)$. In oxalic acid the same tendency was observed in the deformation density of the hydrogen bonds.

The hydrogen bonding in $\text{B}(\text{OH})_3$ was previously investigated theoretically by Yamabe *et al.* (1978). They performed theoretical calculations for the orthoboric acid dimer using an STO-3G minimal basis set. From these computations they conclude that a charge redistribution occurred due to hydrogen bonding, which promotes the hydrogen-bond formation to the neighbouring $\text{B}(\text{OH})_3$ molecules. We undertook more extensive calculations using a double- ζ basis set for the orthoboric acid dimer. The deformation density map for the dimer is shown in Fig. 4(b). This map should be compared with the map calculated with the same basis set for the orthoboric acid monomer by Gupta & Tossell (1981). The deformation density of the dimer looks as if it were composed of the density of two boric acid monomers. However, some small differences could be observed for the O lone pairs taking part in the hydrogen bonding. The maximum of the peak is shifted slightly towards the H atom. The redistribution of charge by the hydrogen bonding that was suggested by Yamabe *et al.* (1978) is not supported by our theoretical calculations.

Lunell (1984) has reported a detailed theoretical investigation of the hydrogen bonding in $\text{NaHC}_2\text{O}_4 \cdot \text{H}_2\text{O}$. He concludes that the changes in the deformation density observed as a consequence of hydrogen bonding can be explained primarily as being a superposition effect between donor and acceptor deformation density. The present results for hydrogen bonding in orthoboric acid support this conclusion.

References

- ALMLÖF, J. (1974). USIP Report 74-29. Univ. of Stockholm.
- BAGUS, P. S. (1971). *IBM Res. Rep.* RJ 1077.
- COPPENS, P. (1982). *Electron Distributions and the Chemical Bond*, edited by P. COPPENS & M. HALL, pp. 61-94. New York: Plenum.
- COPPENS, P. (1984). Project reporter. *Acta Cryst.* A40, 184-195.

- COPPENS, P., LEISEROWITZ, L. & RABINOVICH, D. (1965). *Acta Cryst.* **18**, 1035-1038.
- CRAVEN, B. M. & SABINE, T. M. (1966). *Acta Cryst.* **20**, 214-219.
- CROMER, D. T. & LIBERMAN, D. (1970). *J. Chem. Phys.* **53**, 1891-1898.
- CROMER, D. T. & MANN, J. B. (1968). *Acta Cryst.* **A24**, 321-324.
- DAM, J., HARKEMA, S. & FEIL, D. (1983). *Acta Cryst.* **B39**, 760-768.
- DUNNING, T. H. (1970). *J. Chem. Phys.* **53**(7), 2823-2833.
- DUNNING, T. H. (1971). *J. Chem. Phys.* **55**(2), 716-723.
- GAJHEDE, M. (1985). *Chem. Phys. Lett.* **120**, 266-271.
- GUNDERSEN, G. (1981). *Acta Chem. Scand. Ser. A*, **35**, 729-731.
- GUPTA, A. & TOSSELL, J. A. (1981). *Phys. Chem. Miner.* **7**, 159-164.
- HANSEN, N. K. & COPPENS, P. (1978). *Acta Cryst.* **A34**, 909-921.
- HERMANSSON, K. (1984). Thesis, Univ. of Uppsala.
- HIRSHFELD, F. L. (1976). *Acta Cryst.* **A32**, 239-244.
- International Tables for X-ray Crystallography* (1974). Vol. IV, Table 2.2D. (Present distributor D. Reidel, Dordrecht.)
- JOHNSON, C. K. (1976). *ORTEP*II. Report ORNL-5138. Oak Ridge National Laboratory, Tennessee.
- KIRFEL, A., WILL, G. & STEWART, R. F. (1983). *Acta Cryst.* **B39**, 175-185.
- LUNELL, S. (1984). *J. Chem. Phys.* **80**, 6185-6193.
- REES, B. (1977). *Isr. J. Chem.* **16**, 180-186.
- RETRUP, S. & SARMA, C. R. (1977). *Theor. Chim. Acta*, **46**, 73-77.
- SEILER, P., SCHWEIZER, W. B. & DUNITZ, J. D. (1984). *Acta Cryst.* **B40**, 319-327.
- STEWART, J. M. (1976). Editor. The X-RAY76 system. Tech. Rep. TR-446. Computer Science Center, Univ. of Maryland, College Park, Maryland.
- STEWART, R. F. (1976). *Acta Cryst.* **A32**, 565-574.
- STEWART, R. F., DAVIDSON, E. R. & SIMPSON, W. T. (1965). *J. Chem. Phys.* **42**, 3175-3187.
- SWAMINATHAN, S., CRAVEN, B. M., SPACKMAN, M. & STEWART, R. F. (1984). *Acta Cryst.* **B40**, 398-404.
- YAMABE, S., KITaura, K. & NISHIMOTO, K. (1978). *Theor. Chim. Acta*, **47**, 111-131.
- ZACHARIASEN, W. H. (1954). *Acta Cryst.* **7**, 305-310.

Acta Cryst. (1986). **B42**, 552-557

Deformation Density in Magnesium Sulfite Hexahydrate

BY J. W. BATS, H. FUESS AND Y. ELERMAN*

Institut für Kristallographie und Mineralogie der Universität Frankfurt am Main, Senckenberganlage 30, D-6000 Frankfurt am Main 1, Federal Republic of Germany

(Received 8 January 1986; accepted 4 July 1986)

Dedicated to the memory of Professor P. P. Ewald

Abstract

The deformation electron density in $\text{MgSO}_3 \cdot 6\text{H}_2\text{O}$ has been determined at 120 K from a combination of X-ray and neutron diffraction data. $M_r = 212.47$, rhombohedral, $R3$, $a = 5.911(1) \text{ \AA}$, $\alpha = 96.25(2)^\circ$, $V = 202.6(1) \text{ \AA}^3$, $Z = 1$, $D_x = 1.742(1) \text{ g cm}^{-3}$, $F(000) = 112$, $T = 120 \text{ K}$. Neutron diffraction: $\lambda = 0.8977 \text{ \AA}$, $(\sin \theta/\lambda)_{\max} = 0.945 \text{ \AA}^{-1}$, $\mu = 1.590 \text{ cm}^{-1}$, $R(F) = 0.038$ for 2228 reflections. X-ray diffraction: Mo $K\alpha$ radiation, graphite monochromator, $\lambda = 0.71069 \text{ \AA}$, $(\sin \theta/\lambda)_{\max} = 1.15 \text{ \AA}^{-1}$, $\mu = 4.70 \text{ cm}^{-1}$, $R(F) = 0.018$ for 3222 observed independent reflections. The non-centrosymmetric space group causes an underestimation of the deformation density when using phase angles from a spherical-atom refinement. A doubly phased difference synthesis assigning phase angles from a multipole refinement to F_{obs} gave a detailed description of the deformation density. The sulfite O atoms carry a negative charge and are considerably expanded compared with free atoms. An

extended lone-pair lobe is observed at the apex of the S pyramid. The net charge on the sulfite group is estimated as $-1.0(2) e$. Dipole moments of the hydrate groups derived from the multipole coefficients are $2.37(14)$ and $2.15(14) \text{ D}$ ($1 \text{ D} = 3.3 \times 10^{-30} \text{ C m}$). The shape of the hydrate O lone-pair lobes is clearly affected by cation and hydrogen-bond interactions.

Introduction

The present work is part of our study of the deformation density in sulfates and related compounds. Experimental results on $\text{Na}_2\text{S}_2\text{O}_3$ and $\text{MgS}_2\text{O}_3 \cdot 6\text{H}_2\text{O}$ have been reported previously (Elerman, Bats & Fuess, 1983; Bats & Fuess, 1986). A qualitative comparison with theoretical density maps was presented elsewhere (Fuess, Bats, Cruickshank & Eisenstein, 1985). In this paper we present our results on a sulfite: $\text{MgSO}_3 \cdot 6\text{H}_2\text{O}$. Its crystal structure was first described by Flack (1973) and recently refined by a neutron diffraction study at room temperature (Andersen & Lindqvist, 1984). The present work is based on X-ray and neutron diffraction data measured at 120 K.

* Permanent address: Department of Physics, Faculty of Science, University of Ankara, Beselyer-Ankara, Turkey.